Determination of K_S^0 Fragmentation Functions including BESIII Measurements and using Neural Networks

Maryam Soleymaninia

Institute for Research in Fundamental Sciences (IPM), Iran

Based on: Phys. Rev. D 110, 014019 – Published 12 July 2024

In Collaboration with:
Hadi Hashamipour, Maral Salajegheh, Hamzeh Khanpour, Hubert Spiesberger and Ulf-G. Meißner

Fragmentation Functions (FFs)

FFs are a fundamental ingredient in the framework of QCD, to calculate the cross section for any process that involves the measurement of a hadron in the final state.

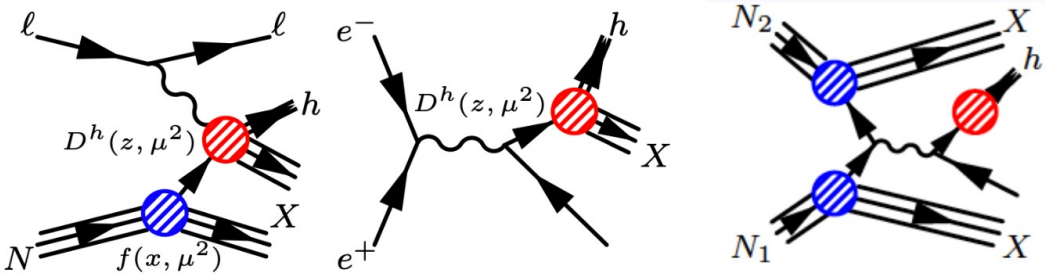

$$\sigma^{\ell N \to \ell h X} = \hat{\sigma} \otimes PDF \otimes FF$$

$$\sigma^{e^+e^- \to hX} = \hat{\sigma} \otimes FF$$

$$\sigma^{pp \to hX} = \hat{\sigma} \otimes PDF \otimes PDF \otimes FF$$

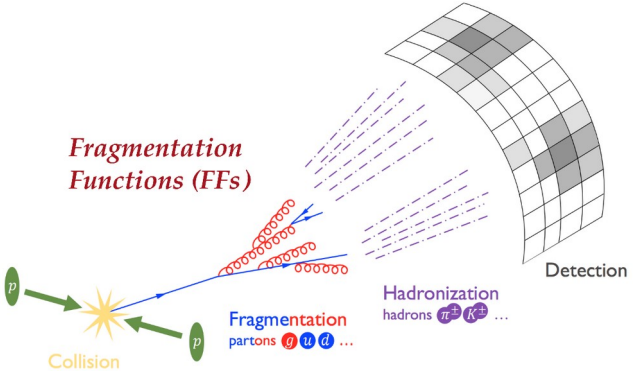

What fraction of the initial parton momentum are carried by hadrons?

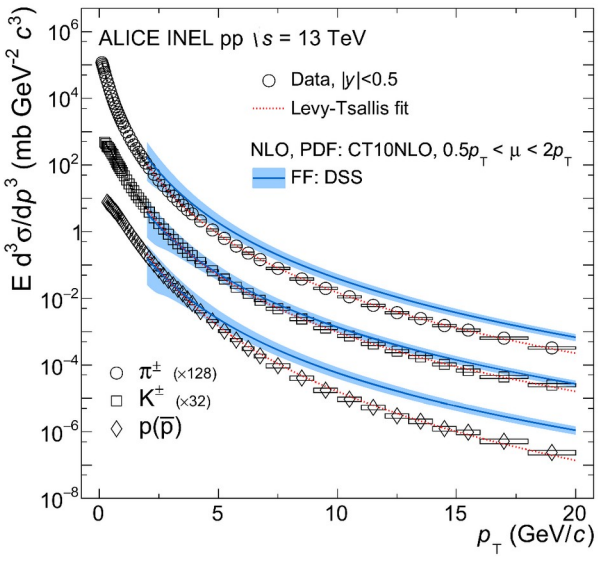

Multi-strange Hadrons

The distribution of hadrons containing strange quarks has been documented at various center-of-mass energies, both at the LHC and at the Tevatron.

- **BKK96:**
  Phys. Rev. D 53, 3573 (1996)
- **AKK05:**
  Nucl. Phys. B 734, 50 (2006)
- **AKK08:**
  Nucl. Phys. B 803, 42 (2008)
- **SAK20:**
  Phys. Rev. D 102, no.11, 114029 (2020)

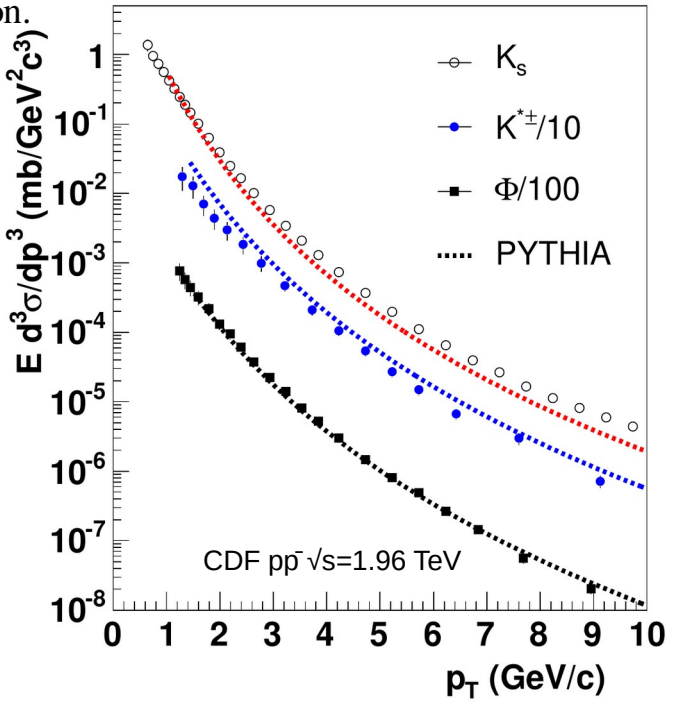

Phys. Rev. D 88, 092005 (2013)

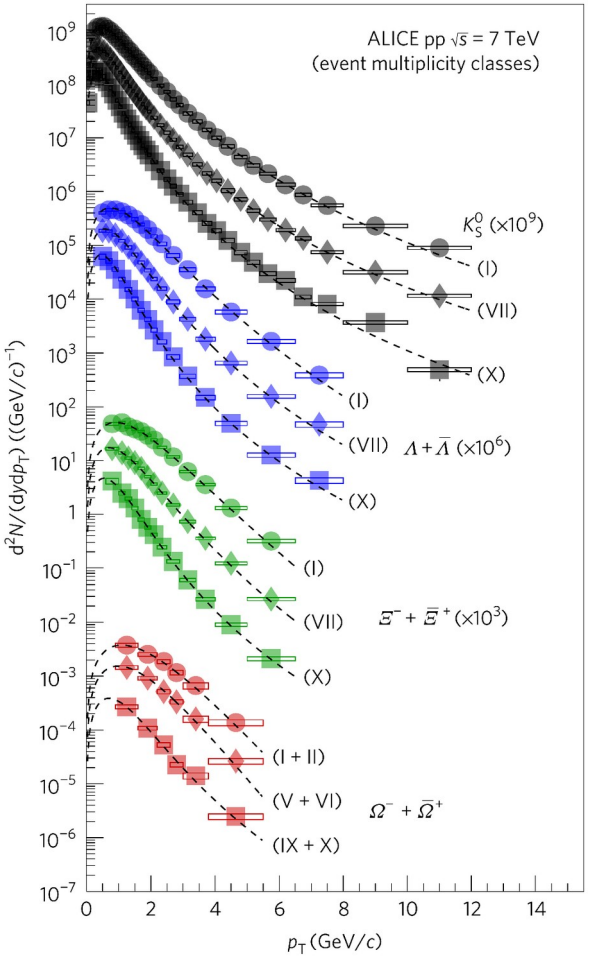

Nature Phys 13, 535–539 (2017).

BESIII Measurements

Beijing Spectrometer(BESIII) Experiment

Phys.Rev.Lett. 130 (2023) 23, 231901

$$z \equiv 2\sqrt{p_h^2 c^2 + M_h^2 c^4}/\sqrt{s}$$

$$\frac{1}{\sigma(e^+e^- \to \text{hadrons})}\frac{\mathrm{d}\sigma(e^+e^- \to h + X)}{\mathrm{d}z_h} = \frac{\sqrt{s}}{2}\sqrt{1 + \frac{M_h^2 c^2}{p_h^2}}\frac{1}{\sigma(e^+e^- \to \text{hadrons})}\frac{\mathrm{d}\sigma(e^+e^- \to h + X)}{\mathrm{d}p_h}$$

$p_{K_S^0}$ (GeV/c)	$\sqrt{s}$ = 2.2324 GeV	$\sqrt{s}$ = 2.4000 GeV	$\sqrt{s}$ = 2.8000 GeV	$\sqrt{s}$ = 3.0500 GeV	$\sqrt{s}$ = 3.4000 GeV	$\sqrt{s}$ = 3.6710 GeV
0.00 – 0.10	0.025 ± 0.004 ± 0.003	0.013 ± 0.002 ± 0.001	0.013 ± 0.002 ± 0.001	0.016 ± 0.002 ± 0.002	0.013 ± 0.005 ± 0.003	0.017 ± 0.004 ± 0.001
0.10 – 0.20	0.108 ± 0.007 ± 0.010	0.113 ± 0.008 ± 0.010	0.098 ± 0.007 ± 0.009	0.094 ± 0.004 ± 0.007	0.077 ± 0.011 ± 0.019	0.103 ± 0.008 ± 0.010
0.20 – 0.30	0.179 ± 0.009 ± 0.009	0.187 ± 0.010 ± 0.014	0.208 ± 0.011 ± 0.015	0.184 ± 0.006 ± 0.019	0.208 ± 0.019 ± 0.041	0.171 ± 0.012 ± 0.021
0.30 – 0.40	0.211 ± 0.010 ± 0.018	0.230 ± 0.011 ± 0.029	0.265 ± 0.012 ± 0.007	0.244 ± 0.007 ± 0.021	0.286 ± 0.021 ± 0.049	0.249 ± 0.014 ± 0.041
0.40 – 0.50	0.195 ± 0.010 ± 0.027	0.214 ± 0.011 ± 0.020	0.254 ± 0.012 ± 0.009	0.246 ± 0.007 ± 0.009	0.253 ± 0.019 ± 0.036	0.252 ± 0.015 ± 0.042
0.50 – 0.60	0.157 ± 0.010 ± 0.005	0.168 ± 0.010 ± 0.017	0.225 ± 0.012 ± 0.029	0.207 ± 0.007 ± 0.011	0.252 ± 0.021 ± 0.025	0.228 ± 0.012 ± 0.036
0.60 – 0.70	0.112 ± 0.008 ± 0.017	0.128 ± 0.009 ± 0.007	0.148 ± 0.009 ± 0.006	0.162 ± 0.006 ± 0.014	0.209 ± 0.017 ± 0.019	0.221 ± 0.012 ± 0.034
0.70 – 0.80	0.076 ± 0.008 ± 0.004	0.088 ± 0.007 ± 0.007	0.126 ± 0.009 ± 0.013	0.124 ± 0.005 ± 0.006	0.145 ± 0.015 ± 0.011	0.165 ± 0.010 ± 0.015
0.80 – 0.90	0.095 ± 0.010 ± 0.006	0.051 ± 0.006 ± 0.005	0.076 ± 0.007 ± 0.005	0.102 ± 0.005 ± 0.006	0.113 ± 0.012 ± 0.005	0.114 ± 0.009 ± 0.015
0.90 – 1.00	–	0.072 ± 0.007 ± 0.008	0.048 ± 0.006 ± 0.005	0.068 ± 0.004 ± 0.005	0.062 ± 0.010 ± 0.007	0.093 ± 0.007 ± 0.005
1.00 – 1.10	–	–	0.043 ± 0.006 ± 0.005	0.047 ± 0.003 ± 0.008	0.046 ± 0.008 ± 0.009	0.060 ± 0.006 ± 0.003
1.10 – 1.20	–	–	0.019 ± 0.004 ± 0.002	0.030 ± 0.003 ± 0.007	0.055 ± 0.009 ± 0.014	0.044 ± 0.005 ± 0.003
1.20 – 1.30	–	–	–	0.014 ± 0.002 ± 0.006	0.020 ± 0.005 ± 0.003	0.026 ± 0.004 ± 0.002
1.30 – 1.40	–	–	–	–	0.019 ± 0.005 ± 0.004	0.020 ± 0.004 ± 0.004
1.40 – 1.50	–	–	–	–	–	0.018 ± 0.003 ± 0.005

This energy range is not well-covered by previous experimental data.

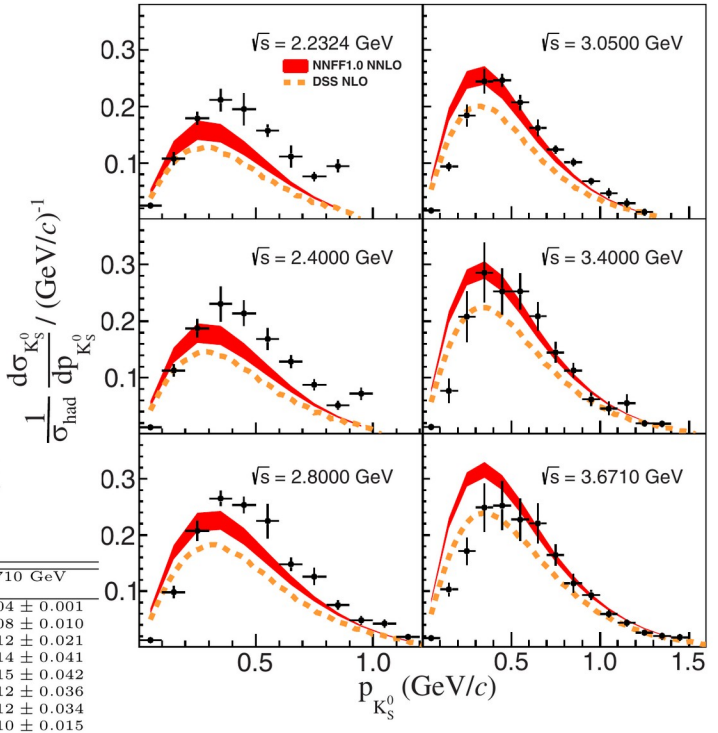

The comparison of the normalized differential cross section of the inclusive production with predictions from NNFF1.0 at NNLO precision and DSS at NLO precision.

Experimental Data

Experiment	Reference	$\sqrt{s}$ GeV	z_{min}	z_{max}
BESIII	[23]	2.2324	0.013	0.8
BESIII	[23]	2.4	0.013	0.8
BESIII	[23]	2.8	0.013	0.9
BESIII	[23]	3.05	0.013	0.9
BESIII	[23]	3.4	0.013	0.9
BESIII	[23]	3.6710	0.013	0.9
TASSO	[27]	14	0.013	0.9
TASSO	[28]	14.8	0.013	0.9
TASSO	[28]	21.5	0.013	0.9
TASSO	[27]	22	0.013	0.9
TPC	[30]	29	0.013	0.9
MARKII	[31]	29	0.013	0.9
TASSO	[27]	34	0.013	0.9
TASSO	[28]	34.5	0.013	0.9
TASSO	[28]	35	0.013	0.9
CELLO	[32]	35	0.013	0.9
TASSO	[28]	42.6	0.013	0.9
TOPAZ	[33]	58	0.013	0.9
ALEPH	[34]	91.2	0.013	0.9
DELPHI	[35]	91.2	0.013	0.9
OPAL	[36]	91.2	0.013	0.9
SLD total	[37]	91.2	0.013	0.9
SLD uds	[37]	91.2	0.013	0.9
SLD charm	[37]	91.2	0.013	0.9
SLD bottom	[37]	91.2	0.013	0.9

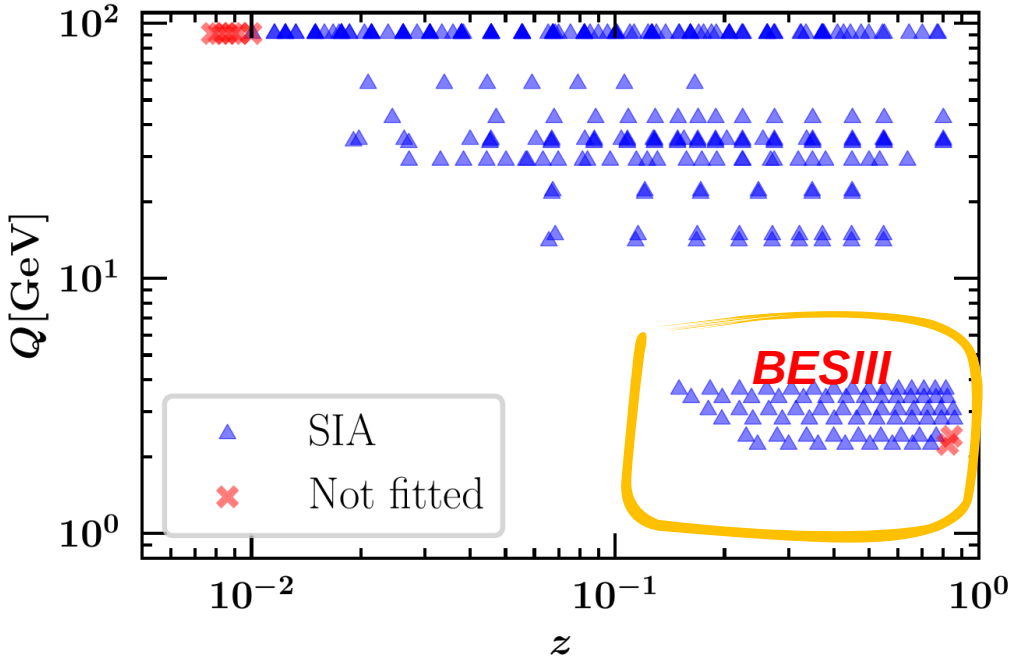

Kinematic range of the experimental SIA data in the (z, Q) plane used to determine the KS0 FFs.

Kinematic cut:
$0.013 \leq z \leq 0.9$

except for two BESIII datasets
Q = 2.2324 and 2.4 GeV

Omitting just 8 data points
$N_{dat} = 346$

Theoretical Setup

Inclusive production of single hadrons

Quarks and hadrons are massless

$$\frac{1}{\sigma_{tot}}\frac{d\sigma^h}{dz} = \frac{1}{\sigma_{tot}} C_i\left(x, \alpha_s(\mu), \frac{Q^2}{\mu^2}\right) \otimes D_i^h\left(\frac{z}{x}, \mu^2\right)$$

FFs

$$z = 2E_h/\sqrt{s}$$

$$C_{ji}\left(z, \alpha_s(\mu), \frac{Q^2}{\mu^2}\right) = (1-\delta_{jL})\delta_{iq}\delta(1-z) + \frac{\alpha_s(\mu)}{2\pi} c_{ji}^{(1)}\left(z, \frac{Q^2}{\mu^2}\right) + \left(\frac{\alpha_s(\mu)}{2\pi}\right)^2 c_{ji}^{(2)}\left(z, \frac{Q^2}{\mu^2}\right) + \cdots,$$

Coefficient functions up to NNLO in pQCD

DGLAP evolution equation

$$\frac{\partial D_i^h(z,\mu^2)}{\partial \ln \mu^2} = P_{ji}\left(x, \alpha_s(\mu^2)\right) \otimes D_j^h\left(\frac{z}{x}, \mu^2\right)$$

Time-like splitting functions

Hadron Mass Corrections

Hadron mass effects are introduced by employing light-cone coordinates and can be taken into account by using a modified scaling variable η instead of z

$$\eta = \frac{z}{2}\left(1+\sqrt{1-\frac{4m_h^2}{sz^2}}\right)$$

Hadron mass

With this change of variables we can express the cross section as

$$\frac{d\sigma}{dz} = \frac{1}{1-m_h^2/s\eta^2}\sum_a \int_\eta^1 \frac{dx_a}{x_a}\frac{d\hat{\sigma}_a}{dx_a} D_a^h\left(\frac{\eta}{x_a},\mu\right)$$

Differential cross section of the hard sub-process with parton a, calculated in pQCD

theory predictions of this work

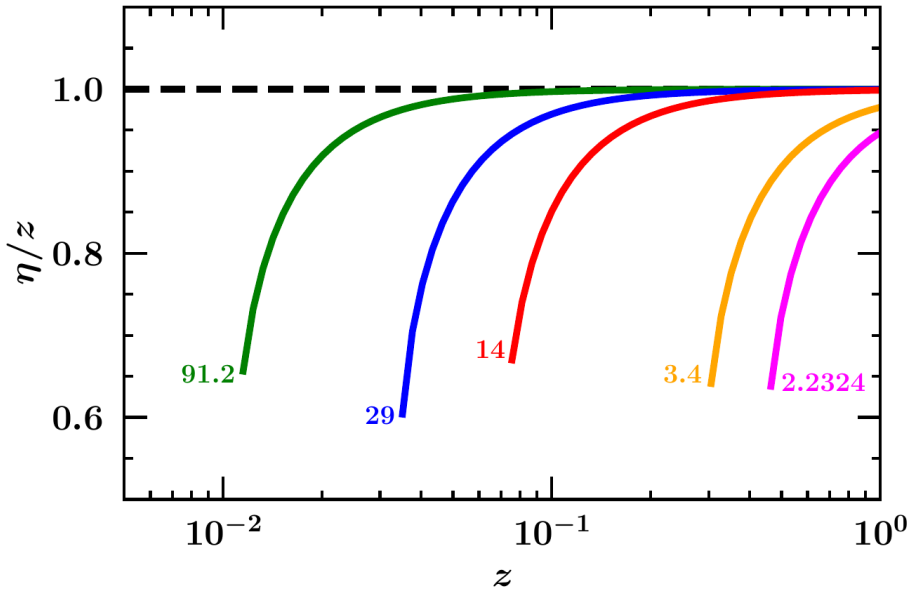

Ratio η/z as a function of z at five representative values of Q.

More details about deriving the formulas:

Eur.Phys.J.A 52 (2016) 10, 316

Neural Network Parametrization

$$zD_i^{h^+}(z,Q_0) = (N_i(z;\boldsymbol{\theta}) - N_i(1;\boldsymbol{\theta}))^2$$

$$D_{u^+}^{K_S^0},\ D_{d^+}^{K_S^0},\ D_{s^+}^{K_S^0},\ D_{c^+}^{K_S^0},\ D_{b^+}^{K_S^0},\ D_g^{K_S^0} \qquad q^+ = q + \bar{q}$$

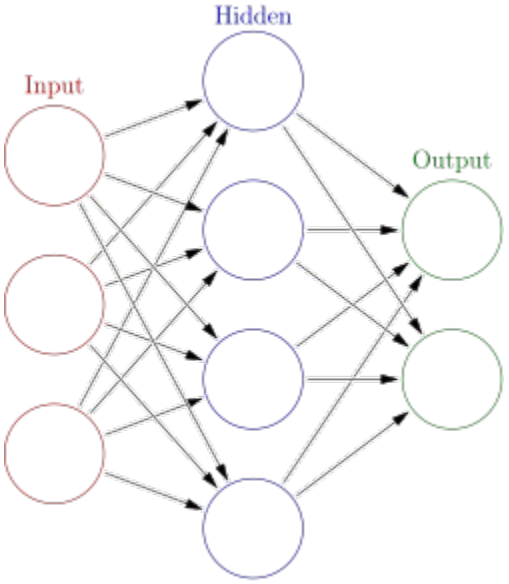

- ✓ *1 node in the input layer which is the value of z*
- ✓ *1 hidden layer, and we pick 25 nodes*
- ✓ *6 output nodes, one for each combination of FFs*

(1 - 25 - 6)

206 parameters
to be fitted to the data

We use the open source framework MontBlanc in all the analyses performed in this work

→ https://github.com/MapCollaboration/MontBlanc

Experimental data and our predictions

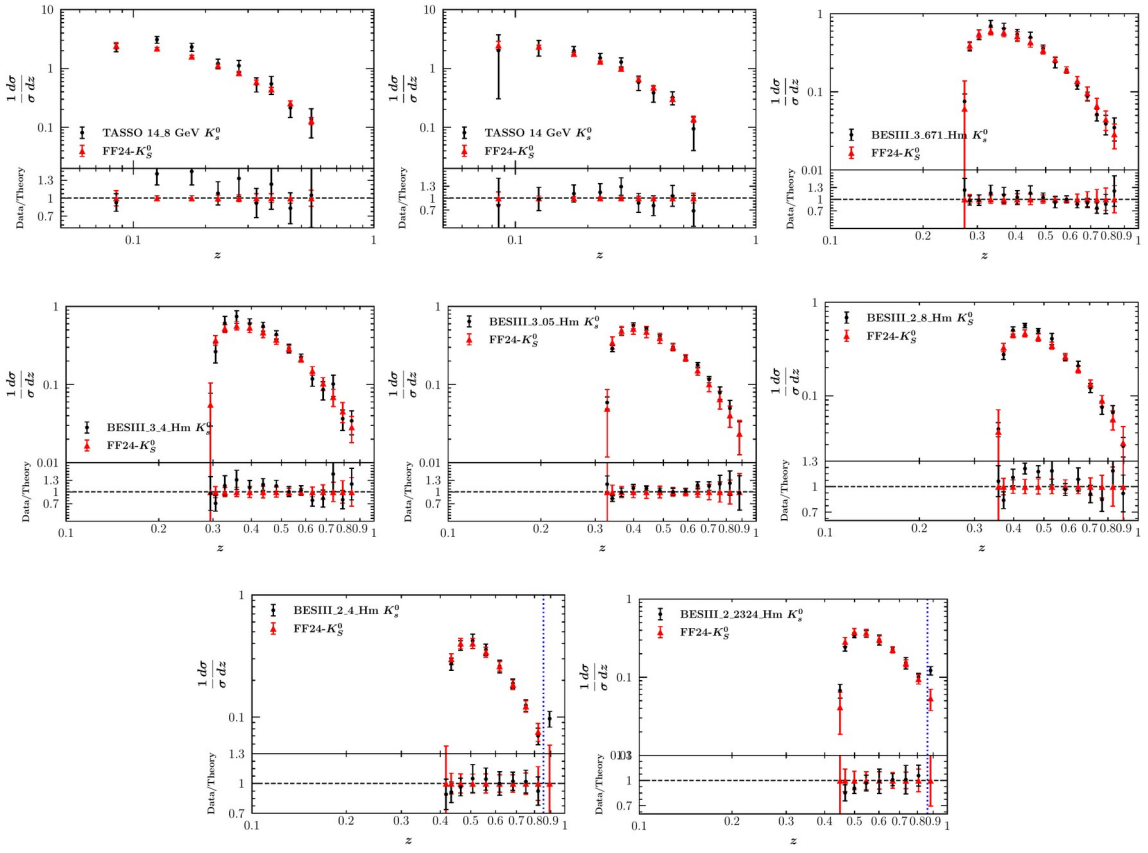

Comparison between the production cross section calculated at NNLO accuracy and experimental data from different experiments. The lower panels show the data/theory ratios.

Experiment	Reference	$\sqrt{s}$ GeV	z_{min}	z_{max}	χ^2_{NLO}/#data	χ^2_{NNLO}/#data
BESIII	[23]	2.2324	0.013	0.8	0.92	0.94
BESIII	[23]	2.4	0.013	0.8	0.14	0.20
BESIII	[23]	2.8	0.013	0.9	2.55	2.18
BESIII	[23]	3.05	0.013	0.9	1.37	1.39
BESIII	[23]	3.4	0.013	0.9	0.84	0.85
BESIII	[23]	3.6710	0.013	0.9	0.55	0.56
TASSO	[27]	14	0.013	0.9	0.68	0.63
TASSO	[28]	14.8	0.013	0.9	1.60	1.55
TASSO	[28]	21.5	0.013	0.9	1.19	1.07
TASSO	[27]	22	0.013	0.9	1.27	1.17
TPC	[30]	29	0.013	0.9	0.23	0.22
MARKII	[31]	29	0.013	0.9	0.37	0.33
TASSO	[27]	34	0.013	0.9	2.04	1.83
TASSO	[28]	34.5	0.013	0.9	1.27	1.21
TASSO	[28]	35	0.013	0.9	0.92	0.85
CELLO	[32]	35	0.013	0.9	0.40	0.35
TASSO	[28]	42.6	0.013	0.9	1.19	1.15
TOPAZ	[33]	58	0.013	0.9	0.34	0.32
ALEPH	[34]	91.2	0.013	0.9	0.35	0.32
DELPHI	[35]	91.2	0.013	0.9	0.70	0.73
OPAL	[36]	91.2	0.013	0.9	0.90	0.88
SLD total	[37]	91.2	0.013	0.9	0.93	0.93
SLD uds	[37]	91.2	0.013	0.9	0.65	0.73
SLD charm	[37]	91.2	0.013	0.9	0.64	0.66
SLD bottom	[37]	91.2	0.013	0.9	1.64	1.46
				Total #data		
Total χ^2/#data				346	0.91	0.87

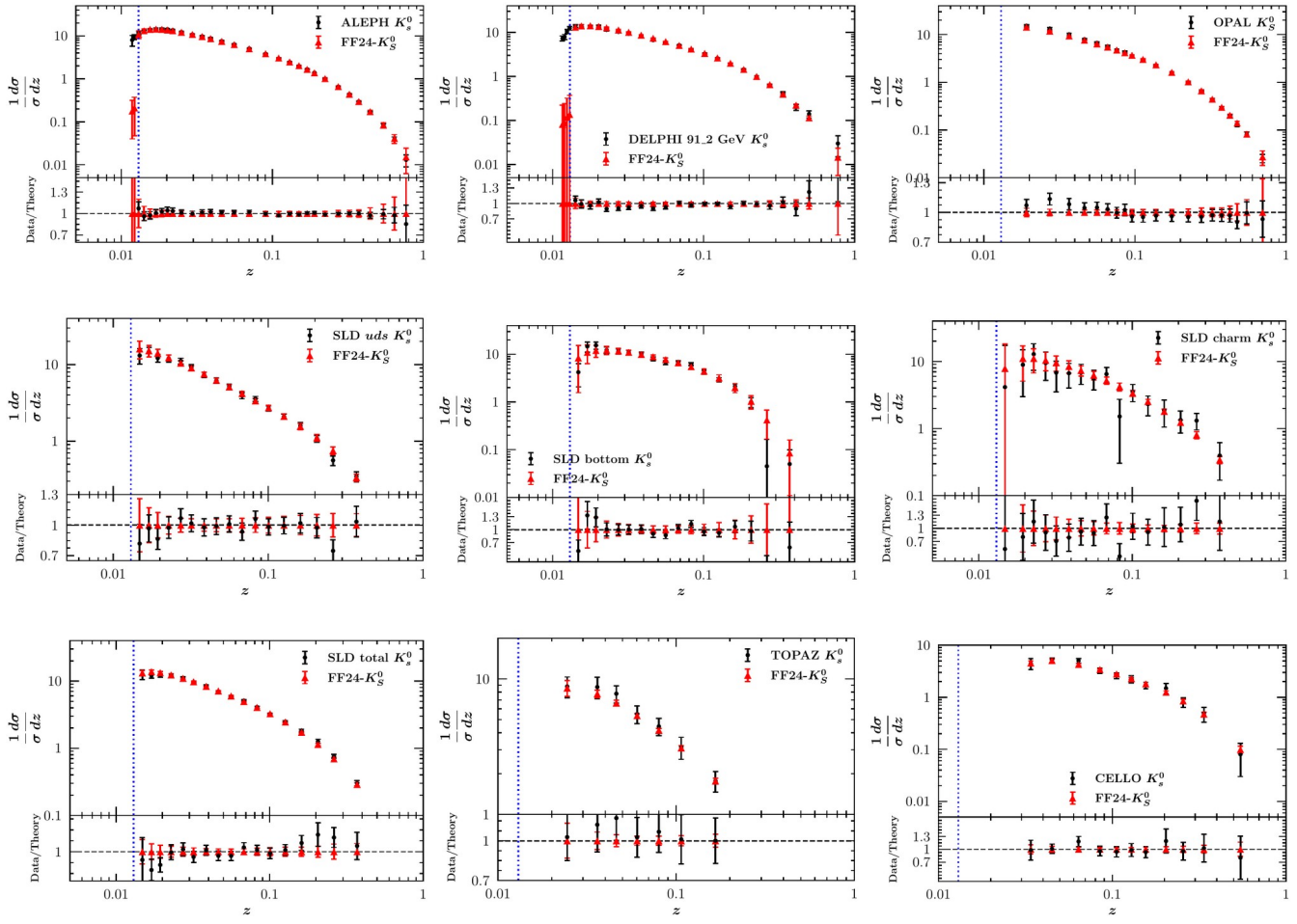

Comparison between the production cross section calculated at NNLO accuracy and experimental data from different experiments. The lower panels show the data/theory ratios.

Comparison FFs

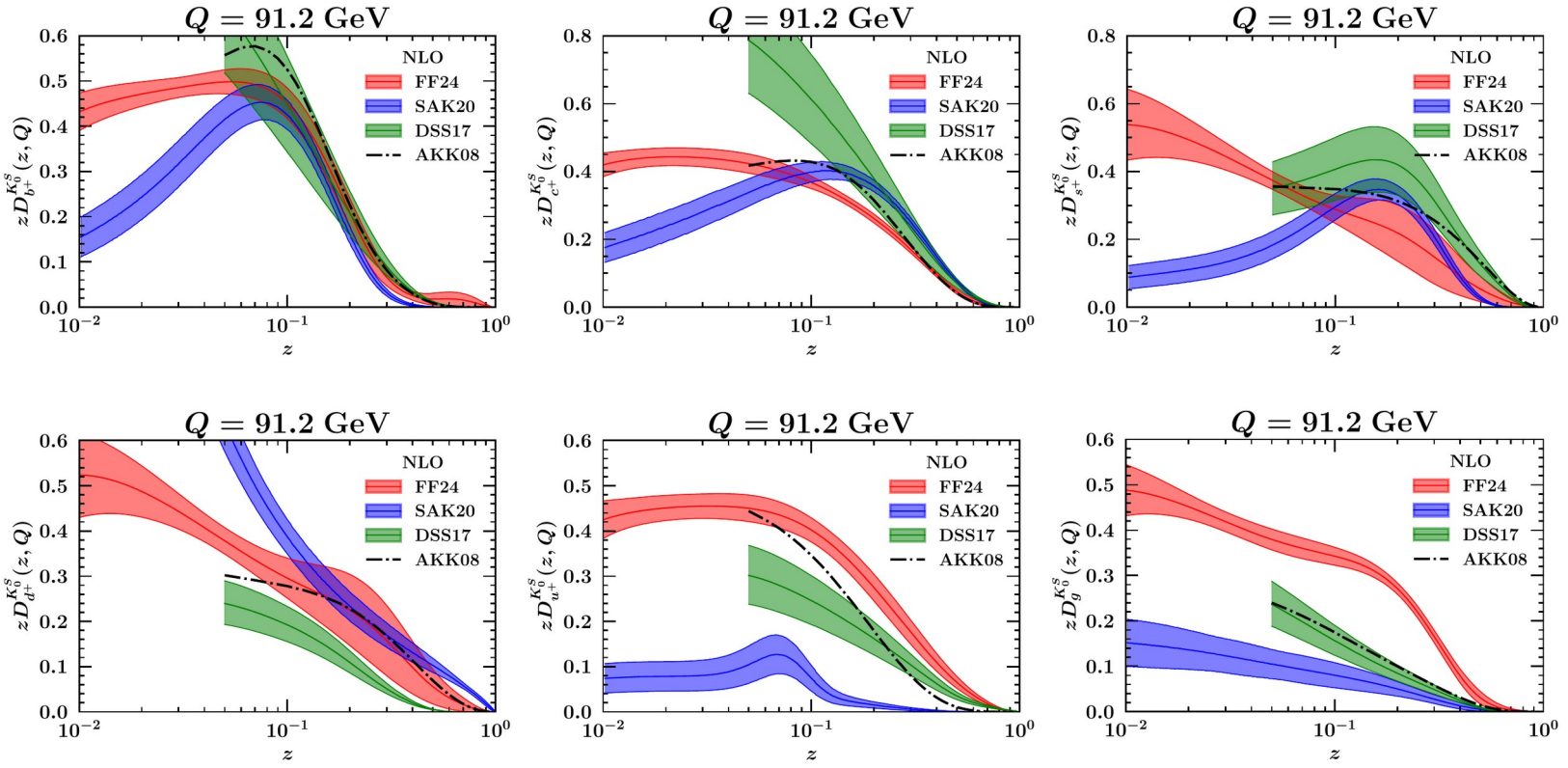

The FF24 at NLO accuracy obtained for various partons at Q = 91.2 GeV. The shaded bands represent estimates derived from the Monte Carlo method. Results from SAK20 [Phys. Rev. D 102, no.11, 114029 (2020)], DSS17 [Phys. Rev. D 95, no.9, 094019 (2017)], and AKK08 [Nucl. Phys. B 803, 42 (2008)] at NLO accuracy are also included for comparison.

Comparison FFs

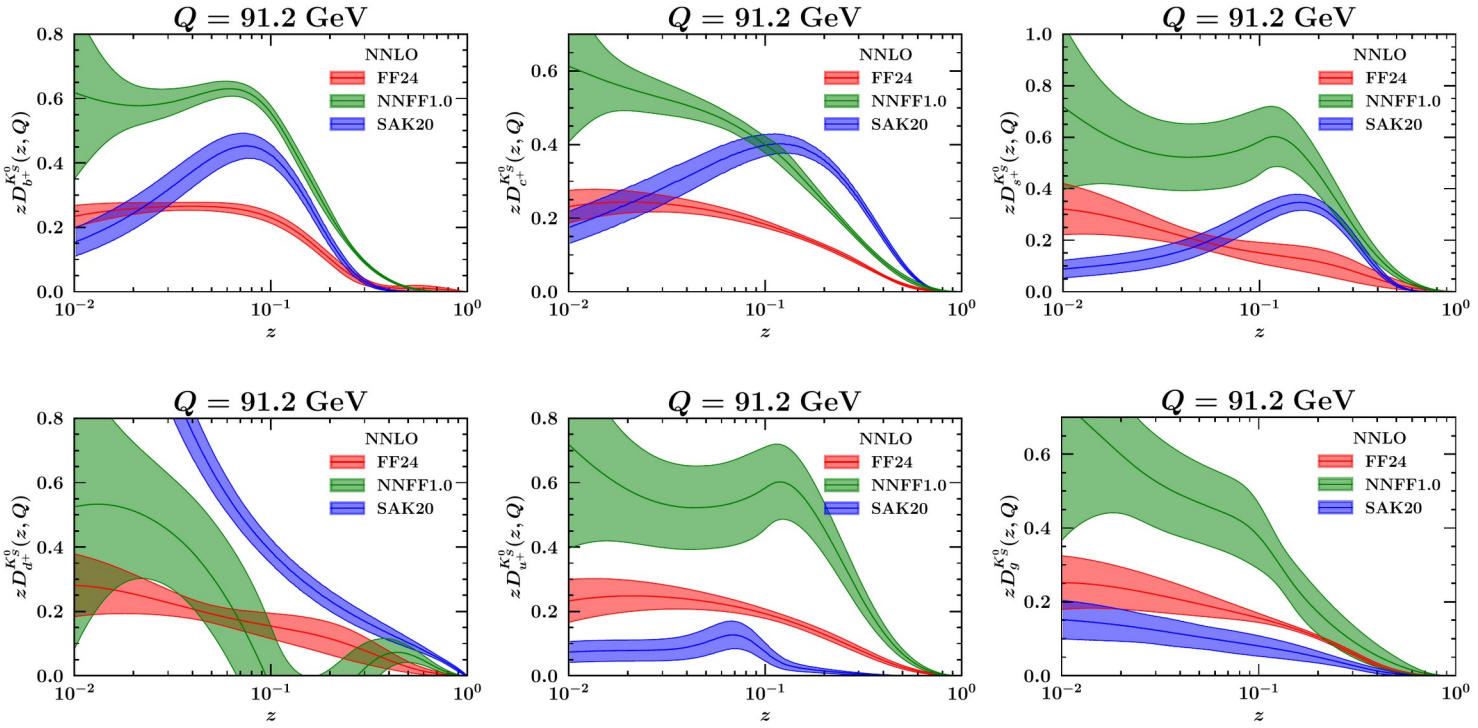

The FF24 at NNLO accuracy obtained for various partons at Q = 91.2 GeV. The shaded bands represent estimates derived from the Monte Carlo method. Results from SAK20 [Phys. Rev. D 102, no.11, 114029 (2020)] and NNFF1.0 [Eur. Phys. J. C 77, no.8, 516 (2017)] are also included for comparison.

SAK20 and FF24- K_S^0

In order to see how the BESIII data affect the determination of FFs, we compare data with predictions obtained from both our previous SAK20 [Phys. Rev. D 102, no.11, 114029 (2020)] FFs and the new FF24- K_S^0 at NLO accuracy .

We observe large differences between data and SAK20 predictions over the full range of z and for all energies.

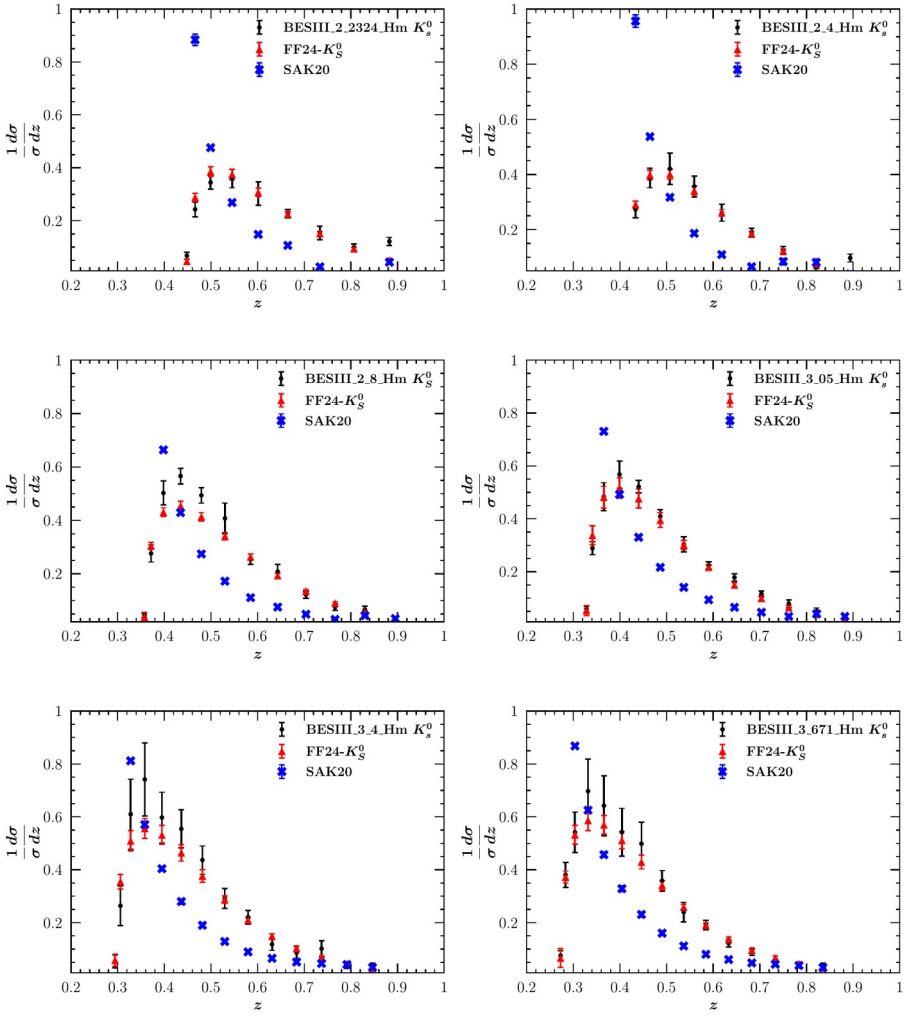

Conclusion

- ✓ **Integration of the latest experimental data from BESIII.**
- ✓ **Focusing exclusively on SIA observables to accurately determine the quark FFs of .**
- ✓ **Utilizing neural networks to parameterize the fragmentation functions, aiming to minimize theoretical bias.**
- ✓ **https://github.com/hashamipour/FF24_K0S_LHAPDF**

Thank You!

Backup

$$F_2^h(z,Q) = \left\langle \hat{e}^2(Q) \right\rangle \Big[C_{2,q}^{\mathrm{S}}\left(z,\alpha_s(Q)\right) \otimes D_{\Sigma}^h(z,Q) + C_{2,q}^{\mathrm{NS}}\left(z,\alpha_s(Q)\right) \otimes D_{\mathrm{NS}}^h(z,Q) + C_{2,g}^{\mathrm{S}}\left(z,\alpha_s(Q)\right) \otimes D_g^h(z,Q) \Big] ,$$

$$D_{\Sigma}^h(z,Q) \equiv \sum_q^{n_f} D_{q^+}^h(z,Q) , \qquad D_{\mathrm{NS}}^h(z,Q) \equiv \sum_q^{n_f} \left(\frac{\hat{e}_q^2}{\langle \hat{e}^2 \rangle} - 1 \right) D_{q^+}^h(z,Q)$$

Quark and antiquark FFs always appear through the combinations. Therefore, SIA measurements are not sensitive to the separation between quark and antiquark FFs.

The leading contribution to the gluon coefficient function C2,gS is O(as), Hence the gluon FF directly enters the fragmentation structure function starting at NLO.

$$\chi^{2(k)} \equiv \left(\mathbf{T}(\boldsymbol{\theta}^{(k)}) - \boldsymbol{x}^{(k)}\right)^{\mathrm{T}} \cdot \mathbf{C}^{-1} \cdot \left(\mathbf{T}(\boldsymbol{\theta}^{(k)}) - \boldsymbol{x}^{(k)}\right)$$

K : replica number

θ : set of weights and biases in NN

T: theoretical prediction

$\boldsymbol{x}^{(k)}$**: Pseudo-data for replica k**

The short-lived neutral kaon is called the K^0_S ("K-short"), decays primarily into two pions, and has a mean lifetime 8.958×10−11 s.

Kaon[2]	K^0	$\overline{K}^0$	$d\bar{s}$	497.611 ± 0.013	½	0^-	1	0	0	[§]	[§]
K-Short[3]	K^0_S	Self	$\frac{d\bar{s}-s\bar{d}}{\sqrt{2}}$ [†][4][5]	497.611 ± 0.013[‡]	½	0^-	[*]	0	0	$(8.954 \pm 0.004) \times 10^{-11}$	$\pi^+ + \pi^-$ or $\pi^0 + \pi^0$
K-Long[6]	K^0_L	Self	$\frac{d\bar{s}+s\bar{d}}{\sqrt{2}}$ [†][4][5]	497.611 ± 0.013[‡]	½	0^-	[*]	0	0	$(5.116 \pm 0.021) \times 10^{-8}$	$\pi^\pm + e^\mp + \nu_e$ or $\pi^\pm + \mu^\mp + \nu_\mu$ or $\pi^0 + \pi^0 + \pi^0$ or $\pi^+ + \pi^0 + \pi^-$

To incorporate the hadron mass effects we use a specific choice of scaling variables. For this purpose, it would be helpful to work with light-cone (L.C) coordinates, in which any four-vector V is written in the form of

$$V = (V^+, V^-, \vec{V}_T)$$

$$V^\pm = (V^0 \pm V^3)/\sqrt{2} \qquad \vec{V}_T = (V^1, V^2)$$

Considering the L.C coordinates, the four-momenta of particles are expressed as

$$q = (\frac{\sqrt{s}}{\sqrt{2}}, \frac{\sqrt{s}}{\sqrt{2}}, \vec{0}), \quad p_H = (\sqrt{2}E_H, 0, \vec{0}),$$

$$x_H = 2E_H/\sqrt{s} \qquad x_H = p_H^+/q^+ \qquad \eta = p_H^+/q^+$$

The variable η is now a more convenient scaling variable for studying hadron mass effects, because it is invariant with respect to boosts along the direction of the hadron's spatial momentum (Z-axis).

While small-z resummation is not explicitly addressed in our present analysis, we acknowledge its importance and plan to explore it in future investigations.

We plan to extend our analysis to include data from the production of K^0_S particles in proton collisions.